THE COLLEGE OF AERONAUTICS

CRANFIELD

THESIS

TITLE: ANALYSIS OF CONVERTIPLANE PROPELLER-ROTORS

AME: F. D. SMITH

DATE: JUNE 1962

18 July 1962

From: LT Frederick D. Smith, Jr., USN, The College of Aeronautics, Cranfield, Bletchley, Bucks., England.

To: Superintendent, U.S. Naval Postgraduate School, Monterey, California

Subj: Thesis, forwarding of

Ref: (a) U.S. Naval Postgraduate School Inst 5000.2A (Ch 1)

Encl: (1) College of Aeronautics Thesis, "Analysis of Convertiplane Propeller-Rotors", by F. D. Smith

1. Encl (1) is forwarded pursuant to the instructions contained in Ref (a).

2. This thesis was prepared as part of the two year course of instruction at the College of Aeronautics, Cranfield, England, leading to a Diploma of the College (D.C.Ae.). A requirement was set by the Department of Aerodynamics that each student produce a satisfactory thesis based on theoretical studies and that students working in small groups produce joint theses based on experimental research. Encl (1) satisfies the former requirement. The thesis satisfying the latter requirement is forwarded with a separate letter.

3. This thesis analyzes the first order effects of aerodynamic design parameters for convertiplane propeller-rotors when operating in hovering and cruising flight, and a criterion for obtaining optimum combinations of these parameters is established.

Very respectfully,

THE COLLEGE OF AERONAUTICS

DEPARTMENT OF AERODYNAMICS

ANALYSIS OF CONVERTIPLANE PROPELLER-ROTORS

by

FREDERICK D. SMITH, JR.
//

Lieutenant

United States Navy

Cranfield, England.

June 1962.

Table of Contents

ANALYSIS OF CONVERTIPLANE PROPELLER-ROTORS

Summary

The need for aircraft with vertical take-off and landing abilities which surpass existing helicopters in cruising speed and range capabilities is established. The current family of VTOL convertiplanes are surveyed and the abilities of the basic types to satisfy specific needs are assessed. It is pointed out that the classes of convertiplanes which use the same propeller-rotor to provide vertical thrust for take-off and landing and horizontal, axial thrust for normal cruising flight can satisfy many of the needs for VTOL convertiplanes.

A basis for evaluation of the performance of propeller-rotors for these convertiplanes is established. It is found that for simple, idealized propeller-rotors which have "ideal twist" for normal cruising flight, optimum performance in hovering is obtained when the propeller-rotor design parameters are such that no collective blade pitch correction is required during hovering.

A functional relation among the propeller-rotor parameters established by the requirement for no collective pitch correction gives rise to a criterion for relating solidity to tip speed for optimum performance.

List of Symbols

A	see equation 4.4(5)
a	the lift curve slope of the propeller-rotor blade section
B	see equation 4.4(6)
b	the number of blades per propeller-rotor
C	see equation 4.4(7)
c	the propeller-rotor blade chord
G	$= \frac{1}{8} a \sigma \omega' R$, a propeller-rotor parameter arising from a natural grouping of its component parameters
k	$= \frac{\omega}{\omega'}$, the ratio of any propeller-rotor angular velocity to the angular velocity used for design point conditions
M_i	the induced figure of merit, defined in section 3.
R	propeller-rotor radius
r	The radial coordinate
s	$= \frac{\rho}{\rho_o}$, the ratio of air density to standard sea-level air density
T	propeller-rotor thrust
V	free stream velocity relative to the propeller-rotor
v	propeller-rotor induced velocity, may be a function of r

v_i momentum theory value of induced velocity, not a function of r

v' propeller-rotor induced velocity at design point conditions, not a function of r

v_o momentum theory value of propeller-rotor induced velocity during hovering

W aircraft gross weight per propeller-rotor

w $= \frac{W}{\pi R^2}$, the propeller-rotor disc loadings

α'_t the incidence of the blade tip section at design point conditions

ϵ $= \frac{T}{W}$, a parameter relating the propeller-rotor thrust to the aircraft weight per rotor, equals unity for hovering and the inverse of the lift-drag ratio for forward flight

$\theta(r)$ the propeller-rotor blade pitch angle relative to the plane of rotation, a function of r

θ'_t the blade pitch angle of the tip section of a propeller-rotor at design point conditions

θ_c a collective correction to the blade pitch angle required to give the desired thrust.

ρ air density

ρ_o standard sea level air density

σ = $\frac{bc}{R}$, propeller-rotor solidity

$\phi(r)$ the in-flow angle, a function of r

ω propeller-rotor angular velocity

subscript o denotes the hovering condition

superscript $'$ denotes design point conditions in normal cruising flight

1. Introduction.

In recent years there has been an increasing interest in aircraft capable of performing vertical take-offs and landings. This interest has undoubtedly been stimulated by the development of the helicopter into an ever more useful vehicle. But as the helicopter has developed, limitations to its future development have become apparent which will be difficult to surmount. Principal among these are its limited cruising speed and limited range.

While efforts to improve helicopter performance are being continued, parallel efforts are now being made to develope various types of convertible aircraft which incorporate vertical lift devices for landings and take-offs, but which rely, in whole or in part, on fixed wings for lift in normal forward flight. One very promising class of such convertiplanes are those in which propeller-rotors tilt, either with or about the wing, to provide vertical thrust for landings and take-offs and horizontal thrust for normal forward flight. It is inherent in the design of such aircraft that the propeller-rotors must operate in extremes of conditions. That is, they must be designed to function efficiently both at large values of static thrust and at relatively low thrust but at high forward speeds.

This thesis proposes a basis for evaluation of the performance of these propeller-rotors, and theoretical investigations are made of the effects of the fundamental design parameters on the performance of idealized simple propeller-rotors. A relation is established between natural groups of the fundamental parameters which assures optimum performance of the propeller-rotors in both the cruising and hovering states.

2. VTOL Aircraft

2.1 Helicopter Capabilities and Limitations

Today helicopters dominate the field of VTOL aircraft. This results quite naturally from their early introduction and the considerable development which has occurred since. But as this development has progressed, it has become increasingly apparent that there are limitations to the future improvement of helicopter performance which will be difficult, if not impossible, to surmount. These are the limits of low cruising speed and short range. R.L. Lichten (Ref. 1) suggests that cruising speeds of only 125 knots may realistically be expected of future helicopters. One of the consequences of such low cruising speeds is a severe limitation of range. A survey of existing helicopters shows that the median quotation for maximum range is only of the order of 400 nautical miles.

Despite these extreme performance limitations, helicopters have proved to be very worthwhile because of their capabilities which have in the past been unique. These are the ability to land and take-off vertically, hover economically, and proceed in well-controlled slow flight. These manoeuvres can be performed by the helicopter with some measure of safety, for even in the event of complete power failure the rotor is a storehouse of

kinetic energy which can be called upon to cushion a forced landing (Ref. 2). And autorotation during descent permits this energy to be maintained until called upon for the landing flare-out.

2.2 Future VTOL Needs

It can be recognized immediately that the two factors which most greatly limit the utility of helicopters, i.e. speed and range, are among the possible virtues of fixed wing aircraft. This question now arises, "Is there a need for an aircraft which combines at least some of the improved speed and range of fixed wing aircraft with the VTOL capability of the helicopter?" Several areas where such hybrid aircraft would prove useful suggest themselves. They are:

1) Search and rescue,
2) anti-submarine warfare,
3) inter-city transport,
4) tactical military transport, and
5) tactical military air support.

2.2.1 Search and Rescue

In most aerial searches today the objects of the search are sighted by fixed wing aircraft because their higher cruising

speed and greater range enables them to search a wide area quickly. But once the object has been sighted it is necessary to call in helicopters or surface assistance to effect a rescue or carry out more detailed investigation. When survivors are the objects of search, they must suffer additional exposure between sighting and ultimate rescue. It would be desirable to have a single aircraft which could effectively perform both the search and rescue phases of such an operation. Hovering ability would be essential. (Ref. 3). Low downwash velocities would be required for the rescue to be effected while hovering. If sufficiently low downwash velocities should prove incompatible with speed and range requirements, provision for open sea landings and take-offs could provide a possible alternate method to retrieve survivors.

2.2.2 Anti-submarine Warfare

The most effective single means of maintaining contact with a submerged submarine is by means of Asdic or Sonar. This equipment must be submerged. Therefore, it is only of practical use to a sea going vessel or hovering aircraft. Helicopters have insufficient speed and range to search a wide area (Ref. 4). An aircraft which had the speed and range to search a wide area

in the manner of fixed wing aircraft, but which could, after detecting a possible submarine, hover to permit localization by means of Asdic or Sonar would be desirable.

2.2.3 Inter-city Transportation

Airlines cannot compete effectively with surface transportation when connecting nearby cities. This is due primarily to the time required for a passenger to proceed from city center to the air terminal and vice versa. But air transport which could operate directly between city centers would eliminate this problem. (Ref. 5). Obviously, expensive property in city centers cannot be converted to airport use for conventional aircraft, but sites could be provided for operation of VTOL aircraft. The prepared landing sites would make low downwash velocities unnecessary, but low downwash velocities might prove desirable from a noise standpoint and for the benefit of ground personnel who may be required in the immediate vicinity of take-off and landing operations. (Ref. 2).

2.2.4 Tactical Military Transport

Existing vertical envelopement schemes require helicopters to operate from advance bases close to front lines. A VTOL

transport with improved speed and range capabilities could operate directly from main supply points well behind front lines. This would make it unnecessary to maintain vulnerable forward bases. Because such a transport would service totally unprepared sites at the front lines, low downwash velocities would be necessary. (Ref. 4). Furthermore, some terrain would prove to be unsuitable for any landings, so some hovering endurance would be desirable.

2.2.5 Tactical Air Support

Modern warfare requires aerial support of ground troops. Tactical support aircraft which are now operational require long smooth runways. Consequently, they are grouped in large numbers at fixed bases which themselves become important military targets. (Ref. 6). VTOL tactical support aircraft which could operate from small sites with either portable landing mats or minimum preparation could be dispersed and better concealed than aircraft which must operate from large fixed bases. Low downwash velocities would be desirable when landing sites are considered, but they are probably not compatible with the basic mission which would require near sonic attack speeds.

2.3 Current VTOL Configurations

The list of VTOL types is nearly as varied as the list of

manufacturers exploring the possibilities of VTOL convertiplanes. The principal types of VTOL convertiplanes now under development or seriously proposed are:

1) unloaded rotor,
2) tilting rotor,
3) tilting wing,
4) deflected slipstream,
5) lifting fans, and
6) lifting jets.

These have been listed in the approximate order of increasing disc loadings and, hence, of increasing downwash velocities.

2.3.1 Unloaded Rotor Convertiplanes

Two examples of the unloaded rotor convertiplane are well known to the Free World. These are the McDonnell XV-1 and the Fairey Rotodyne. Recently the existence of a two rotor design by Kamov has been disclosed by the U.S.S.R., and, still more recently, a new design by Piasecki has been announced. Of the two familiar aircraft of this type, the McDonnell (Ref. 7) and the Fairey, (Ref. 8) both have single rotors powered by tip jets, to which fuel and compressed air are fed through the rotor hub. This method of rotor propulsion reduces rotor torque

transmission to that of the rotor hub friction, thus greatly reducing the control power required in hovering and slow flight. Both aircraft are propelled in forward flight by conventional propellers so that it is unnecessary to tilt the rotor thrust vector as in a helicopter. Small wings partially unload the rotor in forward flight which delays the retreating blade stall permitting slightly higher forward speeds than those of which helicopters are capable. The unloaded rotor concept permits only small speed gains over helicopters, but the low disc loadings possible are compatible with the hovering requirements of some applications.

2.3.2 Tilting Rotor Convertiplanes

Only one notable example of tilting rotor convertiplane has flown. This is the Bell XV-3. (Ref. 2). It has two propeller-rotors mounted at the wing tips which rotate through approximately 90° to provide direct lift for hovering and forward thrust for cruising flight. Propeller-rotor gear ratios are shifted for more efficient cruising in forward flight. This aircraft crashed during its early development when it was equipped with three bladed, fully articulated rotors. But it has since been rebuilt and flown successfully many times using two bladed, semi-articulated rotors.

A different version of the tilting rotor concept is nearly complete in the prototype stage. This is the Curtis-Wright Model 200. It employs four tilting propellers located at the tips of tandem stub wings. The propeller-rotors are three-bladed rigid rotors. These have been designed to give a radial lifting force when in normal cruising flight. The placement of the rotors at each of the four extremities of the aircraft permits control in vertical or hovering flight entirely by differential thrust. The "radial lift force" rotors have been successfully tested on the Curtis-Wright X-100 test bed. The Model 200 is to be a six passenger executive transport of 12,300 pounds gross weight. A larger version designated Model 300 is proposed along similar lines. It would weigh 44,000 pounds and be capable of carrying forty-eight passengers at a 300 knot cruising speed. (Ref. 9).

Intershafting between rotors is required on all current tilting rotor prototypes and proposals.

2.3.3 Tilting Wing Convertiplanes

Tilting wing types seem to be finding the most favor among the prospective tactical military transport types. This is largely due to the Hiller X-18. (Ref. 10). This experimental

prototype by-passed the usual scheme of flying a small, light test bed to study the feasibility of the principal. The X-18 has a gross weight of 33,000 pounds and is capable of a maximum speed of 250 miles per hour. As a result of the experience gained with this project, Hiller, teamed with Ryan and Chance-Vought, have been awarded a contract in an American Tri-Service competition to build five preproduction prototypes of a four engine tilt wing tactical military transport. This aircraft will have a payload capacity of 8000 pounds over a 200-300 nautical mile radius and a cruising speed of 250-300 knots. (Ref. 11).

Vertol built a 3200 pound two rotor tilt wing flying test bed which has flown successfully. (Ref. 12).

All tilt wing convertiplanes experience stability problems when the wing stalls during reconversion to vertical flight. (Ref. 5).

2.3.4 Deflected Slipstream Convertiplanes

The deflected slipstream principal has been used by the Ryan Model 92. (Ref. 13). After twenty-one successful flights the aircraft crashed and is now undergoing rebuilding. Deflected slipstream does not find much favor on its own, but it seems to be

finding favor as a means of augmenting the thrust vectoring ability of tilt wing configurations. (Ref. 5).

Chance-Vought has proposed a ducted fan arrangement which would use ducted fans oriented to provide thrust along the cruising flight path and deflection flaps to vector the thrust for vertical flight. (Ref. 12).

2.3.5 Ducted Fan Convertiplanes

One ducted fan convertiplane is known to have flown. This is the Doak Model 16. (Ref. 14). It has two fixed pitch ducted fans mounted on the wing tips. These fans rotate through 90° to provide lifting thrust for vertical flight and horizontal thrust for forward flight. The aircraft is powered by a shaft-turbine engine. The jet efflux is ducted to the tail where vanes deflect it for pitching and yawing control in vertical and slow flight. This aircraft is known to have made successful conversions between vertical and forward flight. (Ref. 15).

Another ducted fan aircraft is the Vanguard 2C Omniplane. (Ref. 15). This uses three-bladed fans buried in the wings. In forward flight "venetian blinds" close to cover the lower surface and doors close over the upper surface to provide a smooth wing. A pusher propeller provides thrust for forward flight and slipstream

which can be vectored for control during hovering and slow flight. It is not known whether this aircraft has yet flown in free flight. Tethered flight tests were started in 1959.

2.3.6 Jet Lift Convertiplanes

Direct jet lift is incorporated in the Short S.C.1 and in the Hawker P 1127. In the S.C.1, separate engines are used for lift and forward thrust. (Ref. 16). In the P 1127 thrust vectoring from a single engine is used. (Ref. 17). The Hawker configuration appears particularly suitable for a tactical support aircraft. The separate lift engine concept of the S.C.1 is finding favor among advocates of jet lift VTOL transports. It remains to be seen whether the downwash velocities inherent in jet lift can be tolerated for VTOL transports which would fit any of the missions described in paragraph 2.2.

2.4 Mission Compatibility of VTOL Configurations

The needs for VTOL aircraft outlined in paragraph 2.2 can be divided into three basic groups:

1) those in which economic hovering is necessary, e.g., search and rescue or anti-submarine warfare;

2) those in which some hovering endurance is desirable, e.g., the tactical military transport; and

3) those in which hovering ability outside take-off and landing requirements is not necessary, e.g., a tactical support aircraft.

Inter-city transport aircraft would fall in either group two or three. For noise reasons they should probably fall in group two. (Ref. 18). This would also permit an economy in development as both the military tactical transport mission and the inter-city transport mission could be performed by a single suitable basic aircraft.

Group one aircraft require low downwash velocities for economic hovering. For this reason, these aircraft must have low disc loadings. Therefore, either the unloaded rotor or tilting rotor configuration would appear most promising. Tilt wing configurations tend toward higher disc loadings, but they cannot be arbitrarily ruled out without first giving them careful consideration.

Group two aircraft would not require extremely low downwash velocities. Thus, tilt wing or ducted fan aircraft appear as possible choices. Ducted fan experience is still severely limited, so its potential is not known.

Group three applies primarily to tactical support aircraft. The high forward speeds required indicate that jet thrust will be necessary for forward flight. It appears likely then that jet

lift will also be desired, but ducted fans driven by tip turbines are also a possibility. (Ref. 19).

3. VTOL Convertiplanes Using Propeller-rotors

3.1 Potential of Propeller-rotor Convertiplanes

Of several of the principal types of convertiplanes described in Section Two, there are two which are basically similar. These are the tilting rotor and tilting wing configurations. In forward flight, the axes of the rotors of both these types are aligned with the flight path, so that they bear comparatively little resemblance to helicopters and a great deal of resemblance to conventional propeller-driven fixed-wing aircraft. Disc loadings for these types are intermediate between helicopter or rotodyne loadings and those of ducted fans and jet lift. These aircraft can be designed to range in disc loadings from about 10 lb/ft^2 to nearly 100 lb/ft^2. This gives rise to hovering induced velocities ranging from about 45 ft/sec to 145 ft/sec. Induced velocities within this range are compatible with most of the VTOL needs described in Section Two. So these two classes of convertiplane appear to have attractive possibilities.

3.2 Propeller-Rotor Operating Conditions

Since in both the tilting wing and tilting rotor convertiplanes the lifting rotors serve as both rotors and propellers, their operating problems are similar. In hovering flight these propeller-

rotors must produce great static thrust with only the induced flow for inflow. But in forward flight they produce considerably less thrust with a large inflow resulting from the motion of the aircraft. These extremes of operation can cause substantial losses if either operating condition is taken as the design point for the propeller-rotor without giving due consideration to the other operating condition.

3.3 Evaluation of Propeller-Rotor Performance

To evaluate the performance of a propeller-rotor in any given condition, it is necessary to have a basis for comparison. One possible such basis is the ratio of minimum induced power, as determined by momentum theory, to the natural induced power. This ratio shall be defined as "the induced figure of merit", M_i.

$$M_i = \frac{\text{minimum possible induced power}}{\text{actual induced power}} \qquad 3.3(1)$$

In the analysis which follows, a blade element theory will be used for evaluation of the actual induced power, so that equation 3.3(1) becomes

$$M_i = \frac{Tv_i}{\int_o^{R_v} \frac{dT}{dr}\, dr} \qquad 3.3(2)$$

in which T is the total thrust, v_i is the induced velocity computed from momentum theory, and v is the induced velocity computed from blade element theory and may be a function of r. This definition is made for any operating condition which may be considered, so long as both the numerator and denominator reflect the same operating condition.

4. Theoretical Determination of the Induced Figure of Merit

The theory developed in this section relies on the momentum theory of airscrews and simple blade element theory. The development of this theory has been limited to simple idealized propeller-rotors which have constant chord, but which are "ideally twisted" so that the induced velocity at design point conditions is uniform over the disc and equal to the momentum theory value. The dash superscript has been used to denote quantities determined from design point conditions at normal cruise. The subscript zero denotes hovering conditions at sea level.

4.1 Momentum Theory Value of Induced Velocity

From momentum theory, (Ref. 20), it is shown that the thrust of a propeller-rotor is given by

$$T = \rho \pi R^2 (V + v) 2v \qquad 4.1(1)$$

Substituting $\epsilon W = T$ in this equation and solving for v we obtain

$$v = -\frac{V}{2} + \sqrt{\frac{V^2}{4} + \frac{\epsilon W}{2\rho \pi R^2}} \qquad 4.1(2)$$

In this expression W is the gross weight per propeller-rotor of

the aircraft and ϵ is a parameter equal to unity in hovering and equal to the inverse of the lift-drag ratio in horizontal flight. Defining disc loading as $w = \frac{W}{\pi R^2}$ and $\rho = \frac{\rho_o}{s}$ equation 4.1(2) becomes

$$v = -\frac{V}{2} + \sqrt{\frac{V^2}{4} + \frac{sew}{2\rho_o}} \qquad 4.1(3)$$

in which ρ_o is sea level standard density and s is a parameter relating the general density ρ to ρ_o. In hovering, V = 0 and $s = \epsilon = 1$ so

$$v_o = \sqrt{\frac{w}{2\rho_o}} \qquad 4.1(4)$$

In normal cruising flight $\frac{V^2}{4} >> \frac{sew}{2\rho_o}$ and since from equation 4.1(3)

$$v = -\frac{V'}{2} + \frac{V'}{2}\left[1 + \frac{s'\epsilon'w}{2\rho_o} \cdot \frac{4}{V'^2}\right]^{\frac{1}{2}}$$

then

$$v' \doteq \frac{s'\epsilon'w}{2\rho_o V'} \qquad 4.1(5)$$

4.2 Blade Element Theory of Blade Loading

From simple blade element theory, (Ref. 20), the blade loading of one propeller-rotor blade is

$$\frac{dT}{dr} = \frac{1}{2}\rho a c(\omega r)^2 \left[\theta(r) - \phi(r)\right] \qquad 4.2(1)$$

Defining solidity $\sigma = \frac{bc}{\pi R}$, for a propeller-rotor with b blades, equation 4.2(1) becomes

$$\frac{dT}{dr} = \frac{1}{2}\rho a \sigma \pi R(\omega r)^2 \left[\theta(r) - \phi(r)\right] \qquad 4.2(2)$$

The increment of thrust, dT, due to b blade elements of width dr at a general radial distance r is given from equation 4.2(2) by

$$dT = \frac{1}{2}\rho a \sigma \pi R(\omega r)^2 \left[\theta(r) - \phi(r)\right] dr \qquad 4.2(3)$$

The increment of thrust for the annulus of width dr at the same radial position from momentum theory is

$$dT = \rho 2\pi r(V + v)2v\, dr \qquad 4.2(4)$$

Equating 4.2(3) and 4.2(4) we obtain

$$\rho 4\pi r(V+v)v\ dr = \tfrac{1}{2}\rho a\sigma\pi R(\omega r)^2 \left[\theta(r) - \phi(r)\right] dr$$

From which

$$4\pi(V+v)v = \tfrac{1}{2}a\sigma\pi R\omega^2 r \left[\theta(r) - \phi(r)\right] \qquad 4.2(5)$$

From this equation the variation of blade angle, $\theta(r)$, can be determined which will give ideal twist. Since ideal twist is determined by making $\theta(r)$ such that v is independent of r, and since $a\sigma$ has already been taken as independent of r, this can only be accomplished if

$$r\left[\theta'(r) - \phi'(r)\right] = \text{constant} \qquad 4.2(6)$$

(The dash superscript denoting conditions at the normal cruising design point). For axial flow the inflow angle, $\phi(r)$, is given by

$$\phi(r) = \tan^{-1}\frac{V+v}{\omega r} \doteq \frac{V+v}{\omega r} \qquad 4.2(7)$$

Substituting from equation 4.2(7) into 4.2(6)

$$r\left[\theta'(r) - \frac{V'+v'}{\omega r}\right] = \text{constant}$$

and in particular it equals the value at the rotor tip such that

$$r\left[\theta'(r) - \frac{V'+v'}{\omega r}\right] = R\left[\theta'_t - \frac{V'+v'}{\omega R}\right] \qquad 4.2(8)$$

where R is the radius of the propeller-rotor and θ'_t is the blade tip angle. Solving this equation for $\theta'(r)$ we obtain

$$\left.\begin{aligned}\theta'(r) &= \frac{R}{r}\left[\theta'_t - \frac{V'+v'}{\omega R}\right] + \frac{V'+v'}{\omega r} \\ &= \frac{R}{r}\,\alpha'_t + \frac{V'+v'}{\omega r}\end{aligned}\right\} \qquad 4.2(9)$$

where α'_t is the blade incidence at the tip in design point conditions.

Substituting from equations 4.2(7) and 4.2(9) into 4.2(3), we obtain upon integration

$$\begin{aligned}T = \epsilon' W &= \int_0^R \tfrac{1}{2}\rho a\sigma\pi R(\omega' r)^2\left[\frac{R}{r}(\alpha'_t)\right] dr \\ &= \tfrac{1}{4}\frac{\rho_o}{s'} a\sigma\pi R^4\omega'^2\alpha'_t \qquad 4.2(10)\end{aligned}$$

From which

$$\alpha'_t = \frac{4s'\epsilon' W}{\rho_o a\sigma\pi R^4\omega'^2} = \frac{4s'\epsilon' w}{\rho_o a\sigma(\omega' R)^2} \qquad 4.2(11)$$

In general the blade angle, $\theta(r)$, will be given by

$$\theta(r) = \theta'(r) + \theta_c \qquad 4.2(12)$$

where θ_c is a collective pitch correction to the blade angle necessary to give the desired thrust while operating at other than design point conditions. θ_c is constant along the blades and is, therefore, independent of r. Further, in general, the angular velocity, ω, will not necessarily be constant. Therefore the general angular velocity, ω, will be defined as

$$\omega = k\,\omega' \qquad 4.2(13)$$

in which ω' is the angular velocity used for normal cruising. Thus, the general blade loading becomes

$$\frac{dT}{dr} = \frac{1}{2}\rho a \sigma \pi R k \omega' r \left[k\omega' R \alpha'_t + kV' + kv' + k\omega' r\theta_c - (V+v) \right] \qquad 4.2(14)$$

4.3 The Induced Velocity Distribution While Hovering

Replacing equation 4.2(2) by 4.2(14) and working through to equation 4.2(5) we obtain

$$4\pi(V+v)v = \frac{1}{2}a\sigma\pi R k\omega' \left[k(\omega' R\,\alpha'_t + V' + v') + k\omega' r\theta_c - (V+v) \right] \qquad 4.3(1)$$

Therefore

$$(V+v)v = \tfrac{1}{8}a\sigma\omega'Rk\left[k(\omega'R\alpha_t'+V'+v')+k\omega'r\theta_c-(V+v)\right] \qquad 4.3(2)$$

Defining

$$G = \tfrac{1}{8}a\sigma\omega'R \qquad 4.3(3)$$

and

$$H = \omega'R\alpha_t' + V'+v' \qquad 4.3(4)$$

equation 4.3(2) becomes

$$(V+v)v = kG\left[kH+k\omega'r\theta_c-(V+v)\right] \qquad 4.3(5)$$

Solving for v, this becomes

$$(V+v)(v+kG)= kG\left[kH+k\omega'r\theta_c\right]$$

$$v^2+v(V+kG)-kG(kH+k\omega'r\theta_c-V) = 0$$

Therefore

$$v = -\frac{1}{2}(V+kG) + \sqrt{\frac{1}{4}(V+kG)^2+kG(kH+k\omega'r\theta_c-V)} \qquad 4.3(6)$$

which becomes for hovering

$$v = -\frac{k_o G}{2} + \sqrt{\frac{1}{4}(k_o G)^2+k_o G(k_o H+k_o \omega'r\theta_c)} \qquad 4.3(7)$$

4.4 The Collective Pitch Correction

A general expression for the thrust of the propeller-rotor is obtained by integration of equation 4.2(14) over the disc

$$T = \epsilon W = \int_o^R \frac{1}{2}\rho a\sigma\pi Rk\,\omega'r\left[k(\omega'R\,\alpha_t'+V'+v'+\omega'r\theta_c)-(V+v)\right]dr \qquad 4.4(1)$$

Substituting from equation 4.3(3) and 4.3(4), this becomes

$$\epsilon W = \int_o^R 4\,\frac{\rho_o}{s}\pi kGr\left[k(H+\omega'r\theta_c)-(V+v)\right]dr \qquad 4.4(2)$$

For hovering $\epsilon = s = 1$ and $V = 0$ so this becomes

$$W = \int_o^R 4\rho_o\pi k_o Gr\left[k_o(H+\omega'r\theta_c)-v\right]dr \qquad 4.4(3)$$

From equation 4.3(7) it can be seen that v is of the form

$$v = A + \sqrt{B + Cr} \qquad 4.4(4)$$

in which

$$A = - \frac{k_o G}{2} \qquad 4.4(5)$$

$$B = A^2 + k_o^2 GH = k_o^2 \left(\frac{G^2}{4} + GH \right) \qquad 4.4(6)$$

$$C = k_o^2 G \omega' \theta_c \qquad 4.4(7)$$

Therefore

$$v = A + B^{\frac{1}{2}} \left(1 + \frac{C}{B} r\right)^{\frac{1}{2}} \qquad 4.4(8)$$

And since $\frac{C}{B} r$ is much less than unity,

$$v \doteq A + B^{\frac{1}{2}} \left(1 + \frac{C}{2B} r\right) \qquad 4.4(9)$$

Substituting equation 4.4(9) into 4.4(3), we obtain

$$W = 4\pi\rho_o k_o G \int_o^R r\left[k_o H - A - \sqrt{B} + r\left(k_o \omega' \theta_c - \frac{C}{2\sqrt{B}}\right)\right] dr$$

$$= 4\pi\rho_o k_o G \left\{ \frac{R^2}{2}\left[k_o H - A - \sqrt{B}\right] + \frac{R^3}{3}\left[k_o \omega' \theta_c - \frac{C}{2\sqrt{B}}\right] \right\}$$

$$= 4\pi\rho_o k_o G \left\{ \frac{R^2}{2}\left[k_o H - A - \sqrt{B}\right] + \frac{R^3}{3}\left[k_o \omega' \theta_c - \frac{k_o^2 G \omega' \theta_c}{2\sqrt{B}}\right] \right\} \quad 4.4(10)$$

This is an equation in θ_c. Solving for θ_c, this becomes

$$\frac{W}{4\pi\rho_o k_o G R^2} = \frac{w}{4\rho_o k_o G} = \frac{1}{2}\left[k_o H - A - \sqrt{B}\right] + \frac{1}{3}\left[k_o \omega' R \theta_c - \frac{k_o^2 G \omega' R \theta_c}{2\sqrt{B}}\right]$$

$$\therefore \quad \frac{1}{3} k_o \omega' R \theta_c \left(1 - \frac{k_o G}{2\sqrt{B}}\right) = \frac{w}{4\rho_o k_o G} - \frac{1}{2}\left(k_o H - A - \sqrt{B}\right)$$

$$\therefore \theta_c = \frac{3}{k_o \omega' R}\left[\frac{\frac{w}{4\rho_o k_o G} - \frac{1}{2}\left(k_o H - A - \sqrt{B}\right)}{1 - \frac{k_o G}{2\sqrt{B}}}\right] \quad 4.4(11)$$

4.5 The Induced Power Integral

In the preceding paragraphs suitable expressions have been found for all the dependent variables of the induced power integral which appears as the denominator of the induced figure of merit. This can be written for the hovering case

$$I = \int_o^R v \frac{dT}{dr} dr =$$

$$\int_o^R \left[(A + \sqrt{B}) + \frac{C}{2\sqrt{B}} r\right] 4\pi\rho_o k_o G r \left[k_o H - A - \sqrt{B} + r\left(k_o \omega' \theta_c - \frac{C}{2\sqrt{B}}\right)\right] dr \quad 4.5(1)$$

$$I = 4\pi\rho_o k_o G \int_o^R r\left[(A+\sqrt{B})+\frac{C}{2\sqrt{B}}\,r\right]\left[(k_oH-A-\sqrt{B})+r\left(k_o\omega'\theta_c-\frac{C}{2\sqrt{B}}\right)\right]dr$$

$$= 4\pi\rho_o k_o G\left\{\int_o^R (A+\sqrt{B})(k_oH-A-\sqrt{B})\,r\,dr\right.$$

$$+\int_o^R \left[\frac{C}{2\sqrt{B}}\,(k_oH-A-\sqrt{B})+(A+\sqrt{B})\left(k_o\omega'\theta_c-\frac{C}{2\sqrt{B}}\right)\right] r^2\,dr$$

$$\left.+\int_o^R \frac{C}{2\sqrt{B}}\left(k_o\omega'\theta_c-\frac{C}{2\sqrt{B}}\right) r^3\,dr\right\} \qquad 4.5(2)$$

or $I = 4\pi\rho_o k_o G\left(I_1+I_2+I_3\right)$ respectively.

Then

$$I_1 = \int_o^R (A+\sqrt{B})(k_oH-A-\sqrt{B})\,r\,dr$$

$$= \frac{R^2}{2}\,(A+\sqrt{B})(k_oH-A-\sqrt{B}) \qquad 4.5(3)$$

Substituting for A and B, this becomes

$$I_1 = \frac{R^2}{2}\left(-\frac{k_oG}{2}+\sqrt{\frac{k_o^2G^2}{4}+k_oGH}\right)\left(k_oH+\frac{k_oG}{2}-\sqrt{\frac{k_o^2G^2}{4}+k_o^2GH}\right)$$

$$= R^2\,\frac{k_o^2}{2}\left(-\frac{G}{2}+\sqrt{\frac{G^2}{4}+GH}\right)\left(H+\frac{G}{2}-\sqrt{\frac{G^2}{4}+GH}\right) \qquad 4.5(4)$$

Similarly

$$I_2 = \int_o^R \left[\frac{C}{2\sqrt{B}}(k_o H - A - \sqrt{B}) + (A+\sqrt{B})\left(k_o \omega' \theta_c - \frac{C}{2\sqrt{B}}\right) \right] r^2 dr$$

$$= \frac{R^3}{3} \left[\frac{C}{2\sqrt{B}} (k_o H - A - \sqrt{B}) + (A+\sqrt{B})(k_o \omega' \theta_c - \frac{C}{2\sqrt{B}}) \right] \qquad 4.5(5)$$

Substituting for A, B and C, this becomes

$$I_2 = \frac{R^3}{3} \left\{ \left[\frac{k_o^2 G \omega' \theta_c}{2\sqrt{\frac{k_o^2 G^2}{4} + k_o^2 GH}} \right] \left(k_o H + \frac{k_o G}{2} - \sqrt{\frac{k_o^2 G^2}{4} + k_o^2 GH} \right) \right.$$

$$\left. + \left(-\frac{k_o G}{2} + \sqrt{\frac{k_o^2 G^2}{4} + k_o^2 GH} \right) \left(k_o \omega' \theta_c - \frac{k_o^2 G \omega' \theta_c}{2\sqrt{\frac{1}{4}(k_o^2 G^2) + k_o^2 GH}} \right) \right\}$$

$$= R^2 \frac{k_o^2 \omega' R \theta_c}{3} \left[\frac{G}{2\sqrt{\frac{G^2}{4} + GH}} \left(H + \frac{G}{2} - \sqrt{\frac{G^2}{4} + GH} \right) \right.$$

$$\left. + \left(-\frac{G}{2} + \sqrt{\frac{G^2}{4} + GH} \right) \left(1 - \frac{G}{2\sqrt{\frac{G^2}{4} + GH}} \right) \right] \qquad 4.5(6)$$

Finally,

$$I_3 = \int_o^R \frac{C}{2\sqrt{B}} (k_o \omega' \theta_c - \frac{C}{2\sqrt{B}}) \, r^3 dr$$

$$= \frac{R^4}{4} \left[\frac{C}{2\sqrt{B}} \left(k_o \omega' \theta_c - \frac{C}{2\sqrt{B}} \right) \right] \qquad 4.5(7)$$

Substituting for B and C, this becomes

$$I_3 = \frac{R^4}{4}\left[\frac{k_o^2 G\omega'\theta_c}{2\sqrt{\frac{1}{4}(k_o^2G^2)+k_o^2GH}}\left(k_o\omega'\theta_c - \frac{k_o^2G\omega'\theta_c}{2\sqrt{\frac{1}{4}k_o^2G^2+k_o^2GH}}\right)\right]$$

$$= R^2\,\frac{k_o(\omega'R\theta_c)^2}{4}\left[\frac{G}{2\sqrt{\frac{G^2}{4}+GH}}\left(1 - \frac{G}{2\sqrt{\frac{G^2}{4}+GH}}\right)\right] \qquad 4.5(8)$$

4.6 Calculation of the Induced Figure of Merit

All expressions necessary to evaluate the induced figure of merit, M_i, have been determined in terms of the following parameters: air density ratio, blade lift curve slope and solidity, cruising tip speed, ratio of cruising angular velocity to hovering angular velocity, design cruising speed, overall lift-drag ratio at design cruising speed, disc loading, gross weight, and blade radius. Substituting expressions derived in this section, equation 3.3(2) becomes

$$M_i = \frac{Wv_o}{4\pi\rho_o k_o G(I_1+I_2+I_3)} \qquad 4.6(1)$$

4.7 Parametric Groups Affecting the Induced Figure of Merit

In the previous paragraph the many parameters which affect the value of the induced figure of merit were listed. These

parameters do not all exist independently, but rather they occur in natural groups which are always associated together.

Since the integrals I_1, I_2, and I_3 each contain a factor of R^2, equation 4.6(1) can be written

$$M_i = \frac{wv_o}{4\rho_o k_o G\left(\frac{I_1+I_2+I_3}{R^2}\right)} \qquad 4.7(1)$$

The weight per propeller-rotor does not appear independently in any of the remaining terms of this equation, so M_i depends on the disc loading rather than the actual weight.

In equation 4.5(6) and 4.5(8) it can be seen that the integrals I_2 and I_3 contain the term $k_o\omega' R\theta_c$. Equation 4.4(11) shows that the expression for θ_c contains a factor $\frac{1}{k_o\omega' R}$, so that

$$k_o\omega' R\theta_c = 3\left[\frac{\frac{w}{4\rho_o k_o G} - \frac{1}{2}(k_o H - A - \sqrt{B})}{1 - \frac{k_o G}{2\sqrt{B}}}\right] \qquad 4.7(2)$$

Since A and B are functions of $k_o G$ and $k_o H$, the right hand side of this equation contains $k_o\omega' R$ only in these two functions. From equation 4.3(4)

$$k_o H = k(\omega' R\alpha'_t + V' + v')$$

and substituting for α_t' from equation 4.2(11), this becomes

$$k_o H = k_o \left(\frac{4 s' \epsilon' w}{\rho_o a \sigma \omega' R} + V' + v' \right)$$

$$= k_o \left(\frac{k_o s' \epsilon' w}{2 \rho_o k_o G} + V' + v' \right) \qquad 4.7(3)$$

Therefore, the term $k_o \omega' R \theta_c$ contains $\omega' R$ only in the function G, but k_o appears independent of G. Similarly, I_1, I_2, and I_3 contain $\omega' R$ only in the function G, so M_i depends on $\omega' R$ only in the same manner in which it depends on G.

The inverse of the lift-drag ratio, ϵ', and the inverse of the density ratio, s', always occur together as the product $s'\epsilon'$.

This analysis reduces the parameters affecting the induced figure of merit for the hovering comparison to the natural groups G, w, V', $s'\epsilon'$, and k_o.

4.8 Non-dimensional Parametric Groups

The disc loading parameter, w, always appears in the equations divided by the density, ρ_o, so that the combination has the dimensions of velocity squared. G and V' have the dimensions of velocity, and $s'\epsilon'$ and k_o are dimensionless. If the numerator

and denominator of equation 4.7(1) are divided by $k_o^2G^2$, M_i can be expressed as a function of non-dimensional groups of parameters. The result, which is derived in detail in Appendix I, is

$$M_i = \frac{16\left(\frac{w}{2\rho_o k_o^2 G^2}\right)^{3/2} \cdot \left(-\frac{1}{2}+\sqrt{\frac{1}{4}+k_o s'\epsilon'\left(\frac{w}{2\rho_o k_o^2 G^2}\right)+\frac{V'}{G}}\right)}{\left[3\left(\frac{w}{2\rho_o k_o^2 G^2}\right)+\left(-\frac{1}{2}+\sqrt{\frac{1}{4}+k_o^2 s'\epsilon'\left(\frac{w}{2\rho_o k_o^2 G^2}\right)+\frac{V'}{G}}\right)^2\right]^2} \qquad 4.8(1)$$

The non-dimensional groups are $\frac{w}{2\rho_o k_o^2 G^2}$, $\frac{V'}{G}$, and $k_o^2 s'\epsilon'$.

Figure 1 is plotted from equation 4.8(1) for a particular value of $k_o^2 s'\epsilon'$. For all three values of $\frac{V'}{G}$ shown, M_i rises rapidly to a maximum of unity as $\frac{w}{2\rho_o k_o^2 G^2}$ increases. The maxima occur at higher values of $\frac{w}{2\rho_o k_o^2 G^2}$ for higher values of $\frac{V'}{G}$. In each curve, the decrease of M_i is seen to be more gradual beyond the maximum than the rise as $\frac{w}{2\rho_o k_o^2 G^2}$ increases. The parameter $k_o^2 s'\epsilon'$ is normally one or two orders of magnitude less than V'/G. Since this is true, it has relatively little effect on the induced figure of merit except for very large values of $\frac{w}{2\rho_o k_o^2 G^2}$.

5. Maximum Value of the Induced Figure of Merit

5.1 Induced Velocity Distribution When θ_c Vanishes

Equation 4.3(7) is the general expression for the induced velocity distribution while hovering. When the parameters take values such that the collective pitch correction, θ_c, vanishes, this expression becomes

$$v = -\frac{k_o G}{2} + \sqrt{\frac{1}{4}k_o^2 G^2 + k_o^2 GH} \qquad 5.1(1)$$

Since this expression is independent of r, the induced velocity has become constant over the disc. This must, therefore, be identically equal to the momentum theory value for the induced velocity.

5.2 Evaluation of the Induced Power Integral When θ_c Vanishes

Since the induced velocity is constant over the disc when θ_c vanishes, the induced power integral can be written

$$\int_o^R v \frac{dT}{dr}\, dr = v_o \int_o^R \frac{dT}{dr}\, dr \qquad 5.2(1)$$

Therefore, by definition

$$\int_o^R v \frac{dT}{dr}\, dr \equiv v_o T = v_o W \qquad 5.2(2)$$

5.3 The Induced Figure of Merit When θ_c Vanishes

Since the induced power integral becomes identically equal to the momentum theory value of induced power when θ_c vanishes, the induced figure of merit becomes identically unity by equation 3.3(2). The momentum theory gives the least possible value of induced power to produce a given thrust for a specified propeller-rotor. Therefore, the induced figure of merit reaches its maximum value when the collective pitch correction, θ_c, vanishes.

6. Relations Between the Parameters for Maximum Induced Figure of Merit

6.1 Conditions Which Cause θ_c to Vanish

Equation 4.4(11) shows that θ_c will vanish when

$$\frac{w}{4\rho_o k_o G} = \frac{1}{2}(k_o H - A - \sqrt{B}) \qquad 6.1(1)$$

Substituting for A and B this becomes

$$\frac{w}{2\rho_o k_o G} = k_o H + \left(\frac{k_o G}{2} - k_o \sqrt{\frac{G^2}{4} + GH}\right) \qquad 6.1(2)$$

In paragraph 5.1 it was shown that this is equivalent to

$$\frac{w}{2\rho_o k_o G} = k_o H - v_o \qquad 6.1(3)$$

Substituting for H from equation 4.3(4) this becomes

$$\frac{w}{2\rho_o k_o G} = k_o(\omega' R \alpha_t' + V' + v') - v_o \qquad 6.1(4)$$

The induced velocity in forward flight, v', is small compared with V' and will be neglected. Substituting for α_t' and v_o from

equations 4.2(11) and 4.1(4) respectively, we obtain

$$\frac{w}{2\rho_o k_o G} = k_o\left(\frac{4s'\epsilon' w}{\rho_o a\sigma\omega' R} + V'\right) - \sqrt{\frac{w}{2\rho_o}} \qquad 6.1(5)$$

From which

$$\frac{w}{2\rho_o k_o G} = k_o\left(\frac{s'\epsilon' w}{2\rho_o G} + V'\right) - \sqrt{\frac{w}{2\rho_o}}$$

Therefore

$$\frac{w}{2\rho_o k_o G}\left(1 - k_o^2 s'\epsilon'\right) = k_o V' - k_o\sqrt{\frac{w}{2\rho_o k_o{}^2}}$$

finally

$$\frac{w}{2\rho_o k_o^2 G}\left(1 - k_o^2 s'\epsilon'\right) = V' - \sqrt{\frac{w}{2\rho_o k_o{}^2}} \qquad 6.1(6)$$

6.2 Solution for G

Equation 6.1(6) relates the propeller-rotor design parameters which will permit the induced figure of merit to reach unity, its maximum value. That is, combinations of design parameters

which satisfy this equation create a propeller-rotor which is ideally twisted for both the design cruising speed and hovering at the respective thrust loadings, altitudes, and angular velocities.

This equation may be solved to express G as a function of the other parameters

$$G = \frac{\frac{w}{2\rho_o k_o^2}\left(1 - k_o^2 s'\epsilon'\right)}{V' - \sqrt{\frac{w}{2\rho_o k_o^2}}} \qquad 6.2(1)$$

Figure 2 displays G as a function of $\frac{w}{2\rho_o k_o^2}$ for several values of design cruising speed. In figure 2, $k_o^2 s'\epsilon'$ is fixed. This figure shows that G must increase rapidly with disc loading for low forward design speeds, and that G decreases with increasing design speed for a given disc loading. For high cruising speeds at low disc loadings G varies only slightly with either disc loading or speed.

Figure 3 plots G as a function of $s'\epsilon'$ and k_o for a particular design forward speed and disc loading. It shows that G decreases rapidly when k_o increases, and that G decreases slowly and linearly when $s'\epsilon'$ increases.

6.3 Solution for V'

Equation 6.1(6) may be solved for V' to give

$$V' = \frac{W}{2\rho_o k_o^2 G}\left(1 - k_o^2 s'\epsilon'\right) + \sqrt{\frac{W}{2\rho_o k_o^2}} \qquad 6.3(1)$$

This equation specifies the design cruising speed for which ideal twist in forward flight will also be ideal twist in hovering for any combination of the parameters on the right hand side.

Figure 4 shows V' as a function of G and disc loading for a particular k_o and $s'\epsilon'$. It can be seen that, for very low values of G, the design cruising speed must increase rapidly when disc loading increases. Whereas at high values of G, the design cruising speed increases only slowly with disc loading. Thus, for high speeds and low disc loadings, it is necessary to keep G small.

It can be seen from figure 5 that V' is relatively insensitive to changes of $s'\epsilon'$ of reasonable order, but varies rapidly with k_o. V' increases when k_o decreases, and the variation is particularly rapid for the smaller values of k_o.

6.4 Solution for w

If equation 6.1(6) is treated as a quadratic in $\left(\frac{w}{2\rho_o k_o^2}\right)^{\frac{1}{2}}$, we obtain

$$\sqrt{\frac{w}{2\rho_o k_o^2}} = \frac{G}{(1-k_o^2 s'\epsilon')} \left[-\frac{1}{2} + \sqrt{\frac{1}{4} + \frac{V'(1-k_o^2 s'\epsilon')}{G}} \right] \qquad 6.4(1)$$

From which

$$\frac{w}{2\rho_o k_o^2} = \left[-\frac{G}{2(1-k_o^2 s'\epsilon')} + \sqrt{\frac{G^2}{4(1-k_o^2 s'\epsilon')^2} + \frac{V'G}{(1-k_o s'\epsilon')}} \right]^2 \qquad 6.4(2)$$

Therefore

$$w = \rho_o \left[-\frac{k_o G}{(1-k_o^2 s'\epsilon')} + \sqrt{\frac{k_o^2 G^2}{(1-k_o^2 s'\epsilon')^2} + \frac{4k_o^2 V' G}{(1-k_o s'\epsilon')}} \right]^2 \qquad 6.4(3)$$

Figure 6 shows the disc loading as a function of G and V′ for particular values of k_o and $s'\epsilon'$. This figure shows that the disc loading must increase very rapidly as G increases for high design cruising speeds. This increase is much less rapid for low cruising speeds.

In Figure 7 the disc loading is shown as a function of k_o and

$s'\epsilon'$ for particular values of G and design cruising speed. For values of k_o near unity, the disc loading increases only slightly when $s'\epsilon'$ increases; but for higher values of k_o, the disc loading increases rapidly when s increases. For all values of $s'\epsilon'$, the disc loading increases rapidly with increasing k_o.

6.5 Non-dimensional Relation for Maximum Induced Figure of Merit

When both sides of equation 6.1(6) are divided by G, the following non-dimensional equation results

$$\frac{w}{2\rho_o k_o^2 G^2}\left(1 - k_o^2 s'\epsilon'\right) = \frac{V'}{G} - \sqrt{\frac{w}{2\rho_o k_o^2 G^2}} \qquad 6.5(1)$$

From which

$$\frac{V'}{G} = \frac{w}{2\rho_o k_o^2 G^2}\left(1 - k_o^2 s'\epsilon'\right) + \sqrt{\frac{w}{2\rho_o k_o^2 G^2}} \qquad 6.5(2)$$

This equation relates the five basic parametric groups into the same non-dimensional form used in equation 4.8(1). Figure 8 is a plot of this equation which shows $\frac{V'}{G}$ as a function of $\frac{w}{2\rho_o k_o^2 G^2}$ and $k_o^2 s'\epsilon'$. By using the non-dimensional groups of parameters, the information of Figures 2 - 7 are summarized into this one figure.

6.6 Implications of the Parametric Relations

The equations derived in this section, all of which are different forms of equation 6.1(6), relate the basic groups of design parameters in combinations which will provide the maximum induced figure of merit. The parameters of disc loading, cruising speed, lift-drag ratio, and cruising height will probably be fixed by considerations apart from propeller-rotor design. Likewise, the ratio between hovering propeller-rotor angular velocity and cruising angular velocity, k_o, may be fixed by the choice of powerplant or at least confined to narrow limits. The remaining parameter, G, relates the two principal rotor design parameters, solidity and tip speed. When the value of G is fixed by means of the relations established in this thesis, a criterion is established for choosing either the solidity or the tip speed once the other has been fixed. Appendix II provides an example of such use.

7. Conclusions and Recommendations

The ratio between the momentum theory value of induced power and the actual value of induced power is proposed as a measure of the effectiveness of a convertiplane propeller-rotor. This ratio has been defined as "the induced figure of merit".

It was found that, for simple, constant-chord propeller-rotors designed to have "ideal twist" in normal cruising flight, the value of the induced figure of merit reaches unity for certain combinations of design parameters. These combinations occur such that no collective blade pitch correction is required for the off design point operation.

The parameters affecting propeller-rotor design were found to occur naturally in five groups:

1) disc loading,
2) design cruising speed,
3) ratio of hovering to cruising propeller-rotor angular velocity
4) a function of the lift-drag ratio and density ratio; and
5) a function of the blade section lift coefficient, propeller-rotor solidity, and tip speed.

Because the collective blade pitch correction vanishes when the induced figure of merit reaches its maximum, a functional relation was established among these groups of parameters which

provides a criterion for obtaining the maximum value of the induced figure of merit when designing a convertiplane propeller-rotor.

Since the theory contained in this thesis neglects tip effects, finite hub diameters, and variations in planform, it cannot be considered to apply beyond the stage of preliminary design studies. Extension of this thesis to account for these effects is recommended.

References

Ref. 1: The Relative Worth of VTOL Aircraft Types;
Lichten, R.L.
Journal of the American Helicopter Society,
July, 1960, Vol. 5, No. 3, pp 12 - 17.

Ref. 2: XV-3 Low-Disc Loading V/STOL Aircraft Flight Test Experience.
Davis, C.E., and R.L. Lichten.
Aerospace Engineering; August, 1961, Volume 20,
No. 8, pp 22 - 54.

Ref. 3: The Convertiplane, Implications of a New Aircraft type on the National Aviation Policy of The United States. As approved by The Air Coordinating Committee, Washington, D.C.
October, 1954.

Ref. 4: The Place of the Low Disc Loading VTOL in the Future Manned Military Aircraft Spectrum,
Davis, C.E., L.M. Graham, and R.R. Lynn.
Journal of the American Helicopter Society,
January, 1961, Vol. 6, No. 1, pp 22 - 26.

Ref. 5: V/STOL Aircraft - State of the Art, Campbell, John P.
National Aeronautics and Space Administration Technical Note D-624.
January, 1961, pp 3 - 20.

Ref. 6: The Tactical Combat Aircraft:
Towards Total Mobility, Chassin, General L.M. (Ret.).
Interavia, 1961, Vol. XVI, No. 1, pp 54 - 59.

Ref. 7: McDonnel XV-1 Convertiplane,
Coleman, F.
American Helicopter, February, 1954, Vol. XXXIII,
No. 3.

Ref. 8: Fairey Rotodyne, World's First VTOL Commercial
Transport.
Interavia, June, 1958.

Ref. 9: Aviation Week. January 23, 1961, Vol. 74, No. 4,
pp 71 - 76.

Ref. 10: Hiller X-18 Propelloplane,
Berry, M.
American Helicopter, December, 1958, Vol. LIII, No. 1,
pp 6 - 22.

Ref. 11: L-T-V, Ryan, Hiller to Develop Tri-Service VTOL
Transport. Aviation Week. September 25, 1961,
Vol. 75, No. 13, pp 352.

Ref. 12: Vertol 76 Enters Modification Program, Anderton, D.A.
Chance-Vought Studies V/STOL Design, Bulban, E.J.
Aviation Week, October 24, 1960, Vol. 73, No. 17,
pp 56 - 65, pp 71 - 73.

Ref. 13: Ryan Vertiplane, Williams, C. American Helicopter, December, 1957, Vol. XXXXIX, No. 1, pp 10.

Ref. 14: Doak Aircraft Announces Ground Test of New VTOL. American Helicopter, Vol. L, No. 6, May, 1958, pp 12 - 13.

Ref. 15: Ducted Fan VTOL. The Aeroplane and Astronautics, October 2, 1959, Vol. 97, No. 2502.

Ref. 16: The Flat Riser Solution. The Aeroplane, December 13, 1957, Vol. XCIII, No. 2415.

Ref. 17: The Hawker P.1127. Interavia, 1961, Vol. XVI, No. 1, pp 77.

Ref. 18: The Role of Jet Lift, Keith-Lucas, D. The Journal of the Royal Aeronautical Society, May, 1962, Vol. 66, No. 617.

Ref. 19: General Electric Lift Fans. Interavia, 1961, Vol. XVI, No. 1, pp 96.

Ref. 20: Gessow, Alfred and Garry C. Myers, Jr.: Aerodynamics of the Helicopter 1952, First Printing, The Macmillan Company, New York.

Bibliography

Glauert, H.: The Elements of Aerofoil and Airscrew Theory, 1948, 2nd ed., Cambridge University Press.

Gessow, A., and G.C. Meyers, Jr.: Aerodynamics of the Helicopter, 1952, 1st printing, The MacMillan Co., New York.

Shapiro, J.: Principles of Helicopter Engineering, 1955, Temple Press Ltd., London.

Dommasch, D.O.: Elements of Propeller and Helicopter Aerodynamics, 1953, Pitman Publishing Corp., New York.

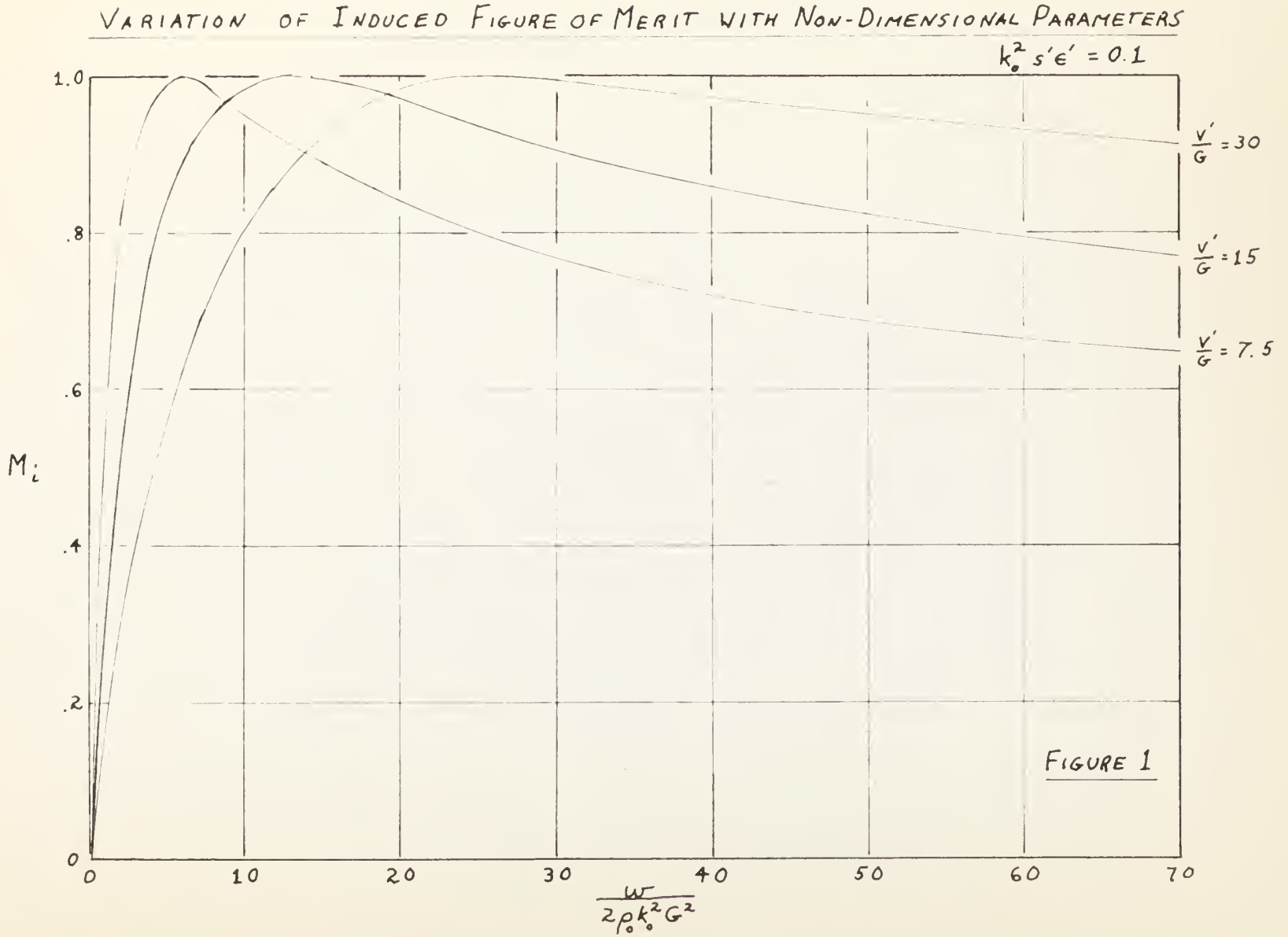
VARIATION OF INDUCED FIGURE OF MERIT WITH NON-DIMENSIONAL PARAMETERS
$k_o^2 s'\epsilon' = 0.1$
$\frac{V'}{G} = 30$
$\frac{V'}{G} = 15$
$\frac{V'}{G} = 7.5$
M_i
1.0
.8
.6
.4
.2
0
0
10
20
30
40
50
60
70
$\frac{W}{2\rho_o k_o^2 G^2}$
FIGURE 1

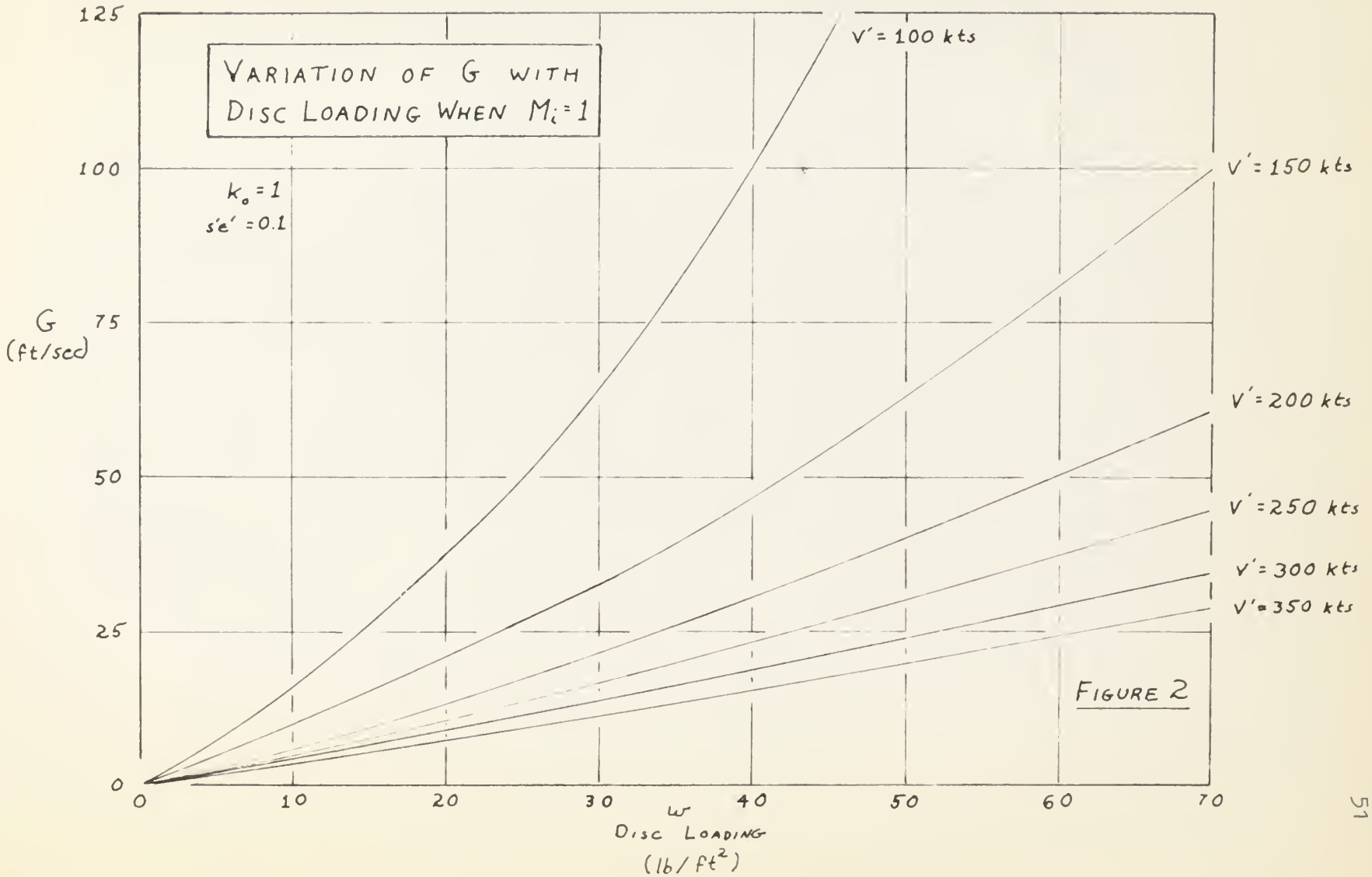
VARIATION OF G WITH DISC LOADING WHEN $M_i = 1$
$k_o = 1$
$s'e' = 0.1$
V' = 100 kts
V' = 150 kts
V' = 200 kts
V' = 250 kts
V' = 300 kts
V' = 350 kts
G (ft/sec)
125
100
75
50
25
0
0
10
20
30
40
50
60
70
w
Disc Loading
(lb/ft²)

FIGURE 2

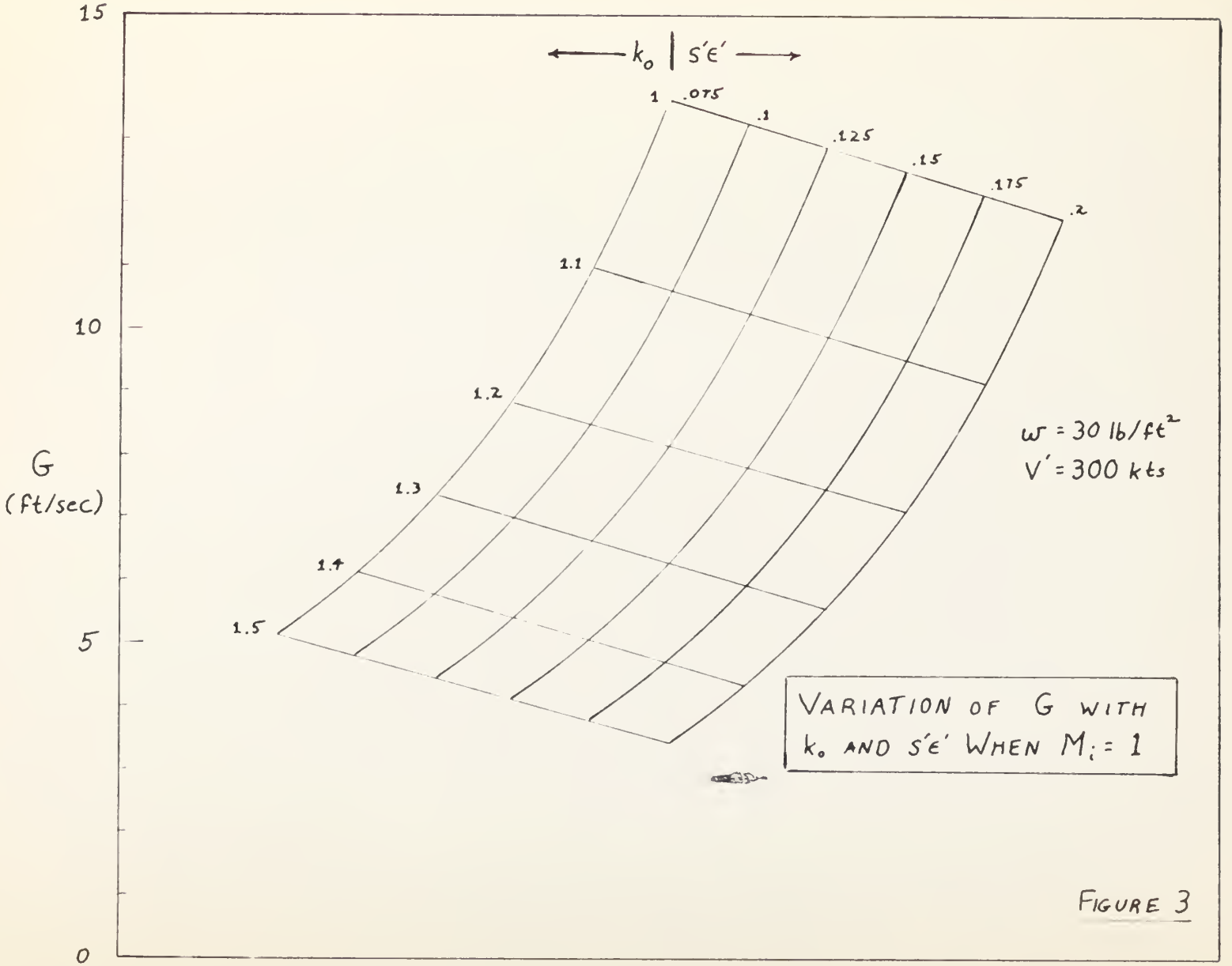
15
10
5
0
G
(ft/sec)
k_o | s'ε'
1
.075
.1
.125
.15
.175
.2
1.1
1.2
1.3
1.4
1.5
$w = 30\ lb/ft^2$
$V' = 300\ kts$
VARIATION OF G WITH k_o AND s'ε' WHEN $M_i = 1$

FIGURE 3

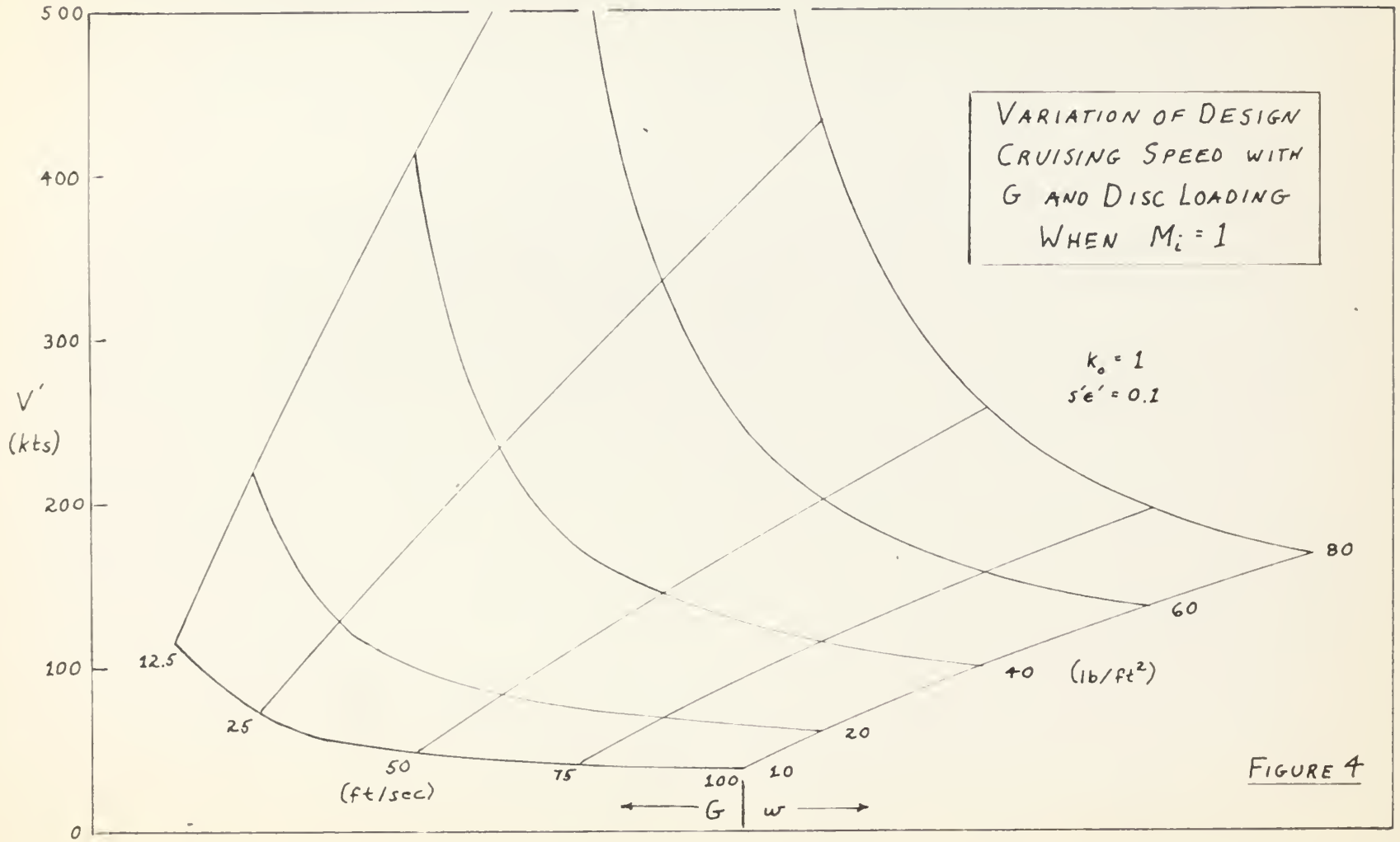
VARIATION OF DESIGN CRUISING SPEED WITH G AND DISC LOADING WHEN $M_i = 1$
$k_o = 1$
$s'\epsilon' = 0.1$
V' (kts)
500
400
300
200
100
0
12.5
25
50
75
100
(ft/sec)
G
10
20
40
60
80
(lb/ft²)
w

FIGURE 4

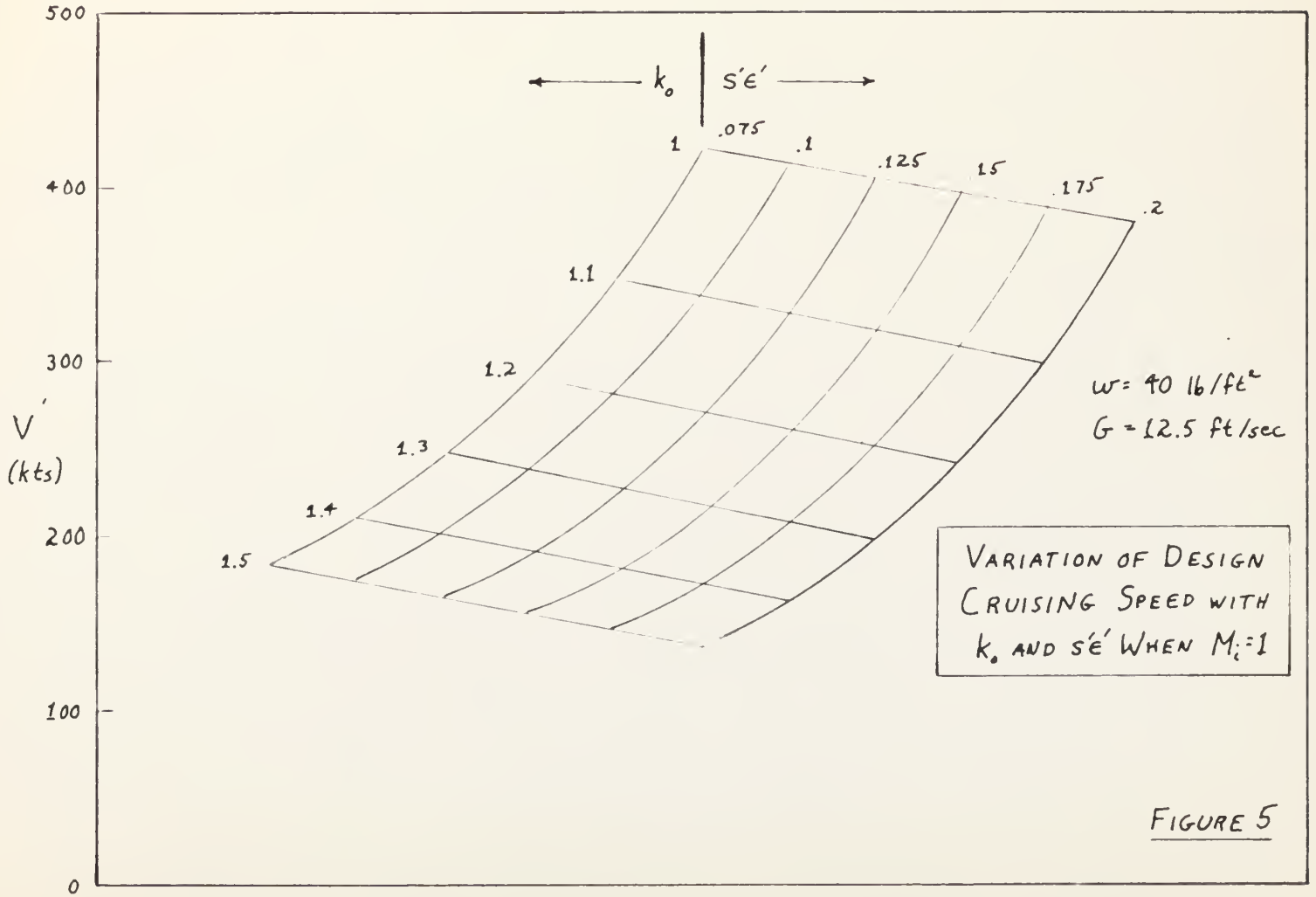

VARIATION OF DESIGN CRUISING SPEED WITH k_o AND s'ε' WHEN M_i = 1

FIGURE 5

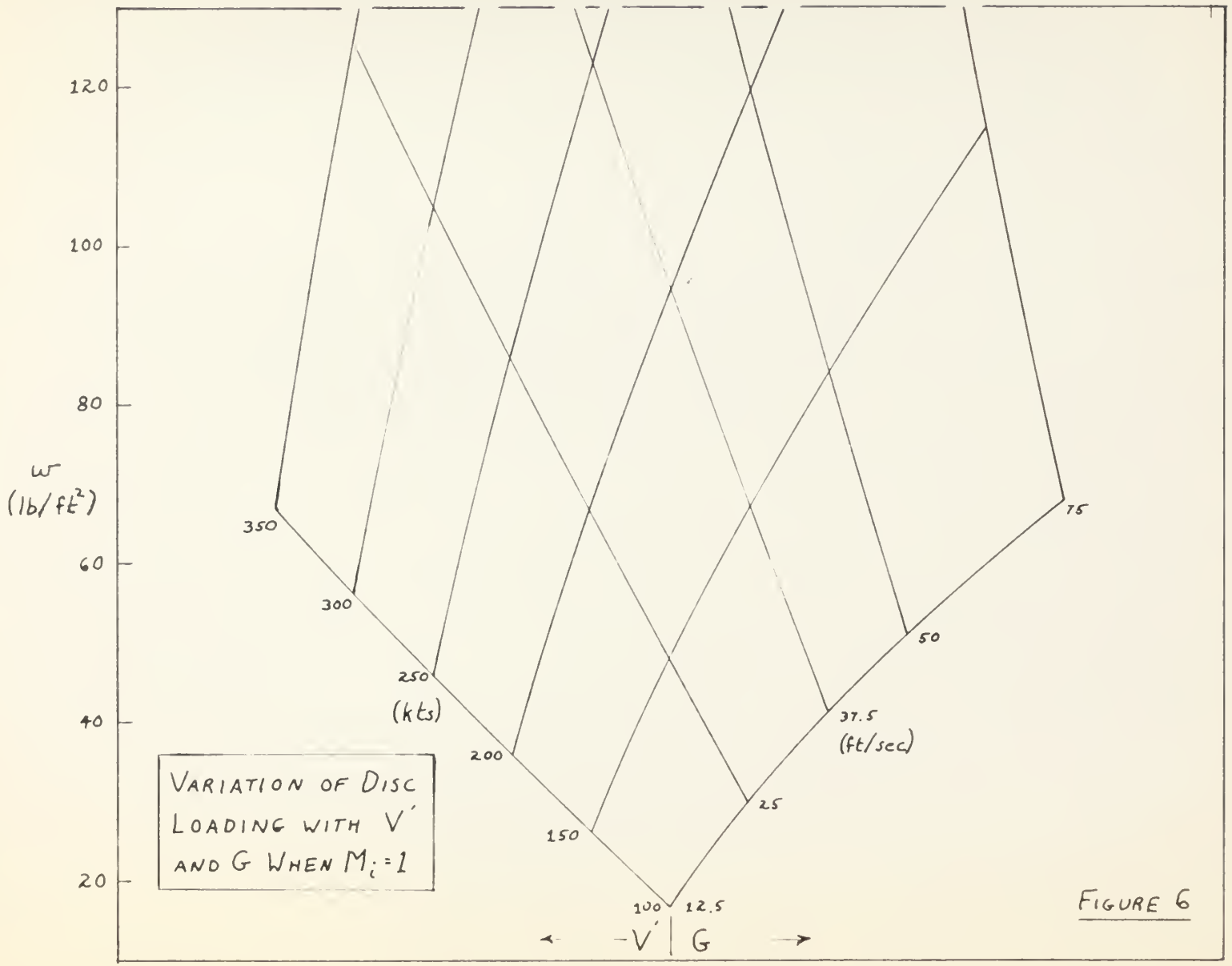
120
100
80
60
40
20
w
(lb/ft²)
350
300
250
(kts)
200
150
100
75
50
37.5
(ft/sec)
25
12.5
-V'
G
VARIATION OF DISC LOADING WITH V' AND G WHEN M_i = 1

FIGURE 6

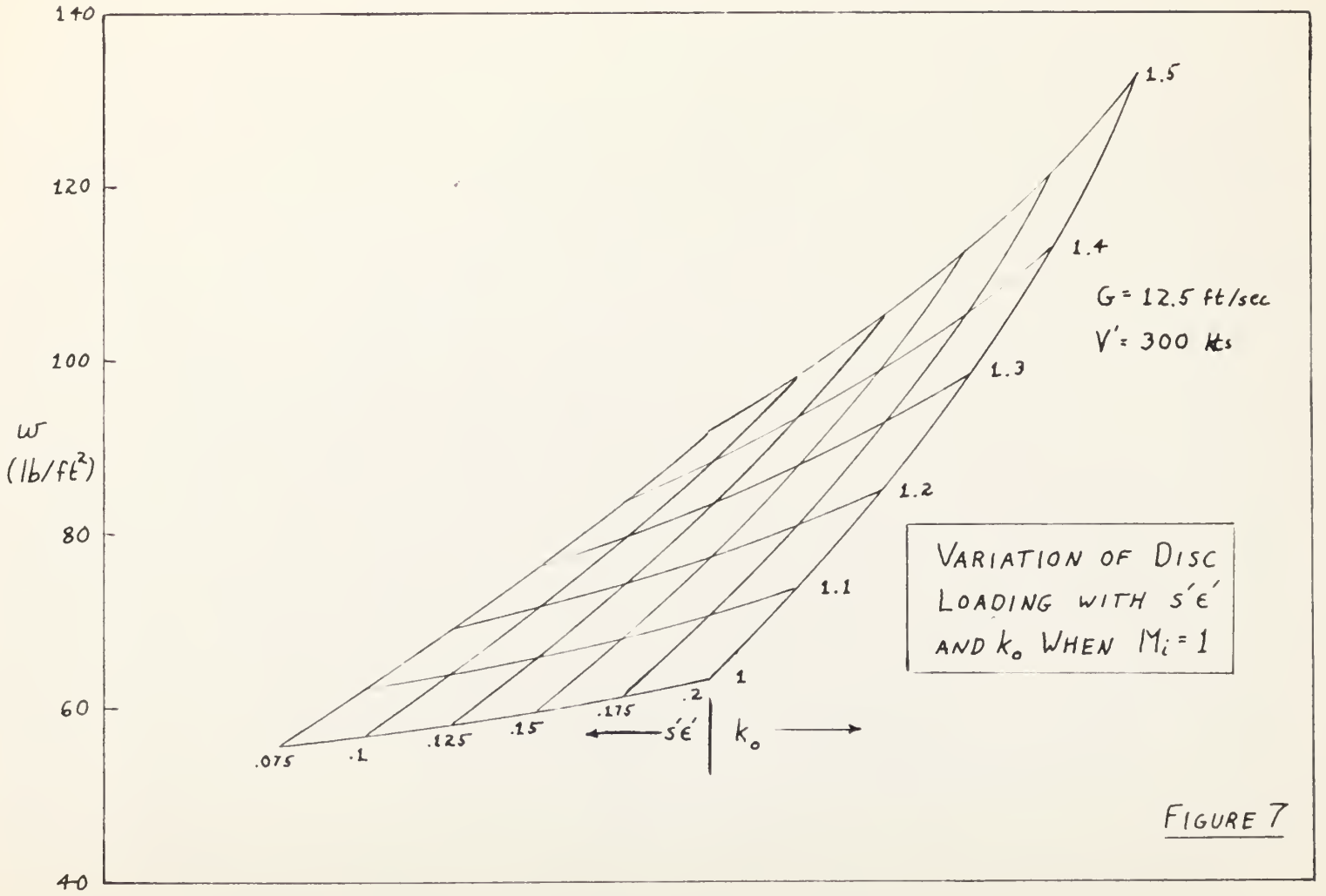
140
120
100
80
60
40
w
(lb/ft²)
1.5
1.4
1.3
1.2
1.1
1
.2
.175
.15
.125
.1
.075
s'ε'
k₀
G = 12.5 ft/sec
V' = 300 kts
VARIATION OF DISC LOADING WITH s'ε' AND k₀ WHEN Mᵢ = 1

FIGURE 7

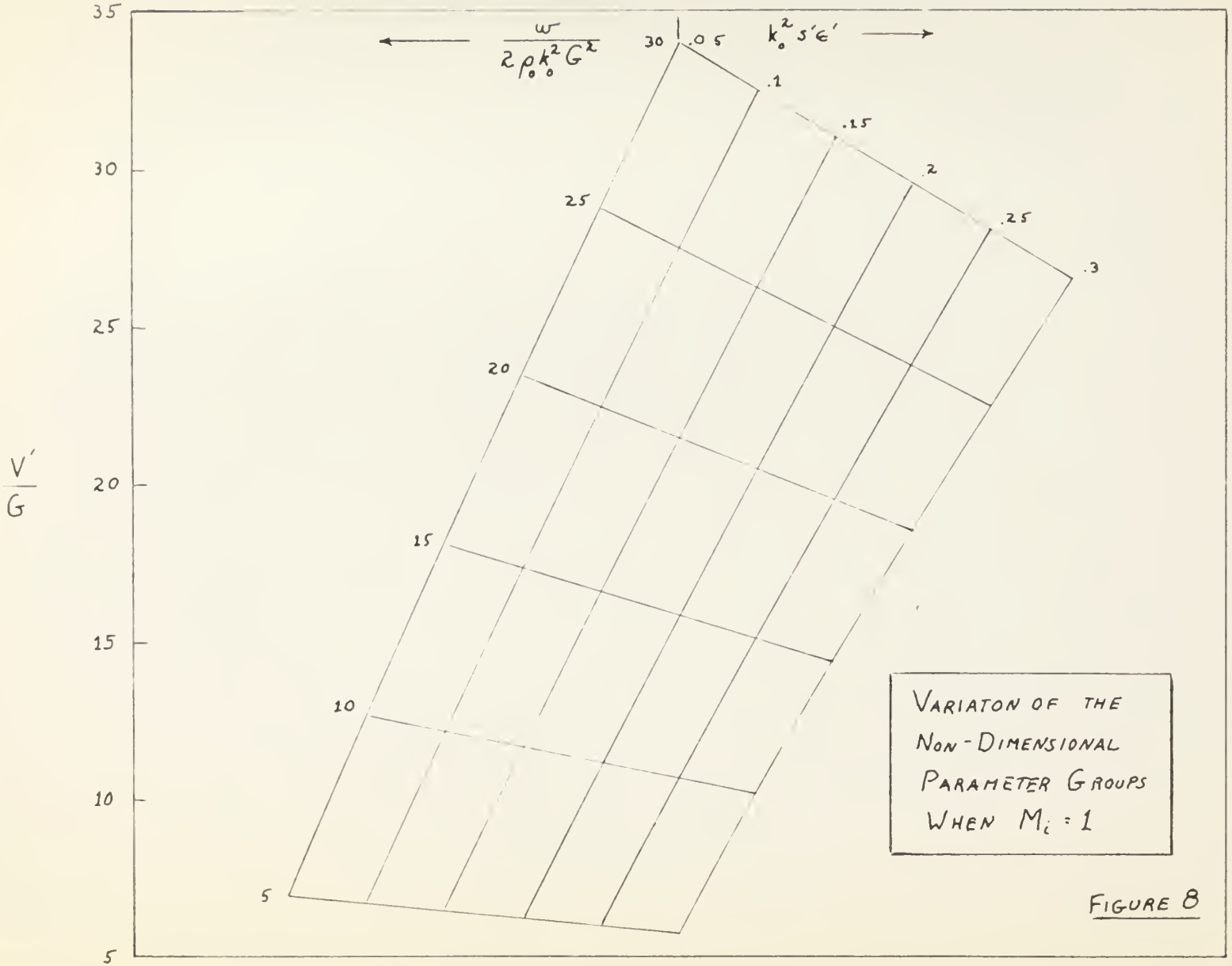
$\frac{\omega}{2\rho_0 k_0^2 G^2}$
$k_0^2 s' \epsilon'$
.05
.1
.15
.2
.25
.3
35
30
25
20
15
10
5
$\frac{V'}{G}$
Variaton of the Non-Dimensional Parameter Groups When $M_i = 1$

FIGURE 8

Appendix I

The Induced Figure of Merit in Terms of Non-dimensional Parameters

I.1 Expressing θ_c in a Non-dimensional Function

Equation 4.7(2) provides an expression for $k_o \omega' R \theta_c$. This quantity has the dimensions of velocity. Dividing both sides of this equation by $k_o G$ puts it into the following non-dimensional form

$$\frac{\omega' R \theta_c}{G} = \frac{3}{2}\left[\frac{\frac{w}{2\rho_o k_o^2 G^2} - \left(\frac{H}{G} + \frac{1}{2} - \sqrt{\frac{1}{4} + \frac{H}{G}}\right)}{1 - \frac{1}{2\sqrt{\frac{1}{4} + \frac{H}{G}}}}\right] \qquad \text{I.1(1)}$$

I.2 Derivation of Equation 4.8(1)

Equation 4.7(1) when rearranged, becomes

$$M_i = \frac{w\, v_o}{4\rho_o k_o G} \cdot \frac{R^2}{(I_1+I_2+I_3)} \qquad \text{I.2(1)}$$

Dividing both the numerator and denominator by $k_o^2 G^2$, this becomes

$$M_i = \frac{w\, v_o}{2\rho_o k_o^3 G^3} \cdot \frac{(k_o G R)^2}{2(I_1+I_2+I_3)} \qquad \text{I.2(2)}$$

Since

$$v_o = \sqrt{\frac{w}{2\rho_o}}$$

from equation 4.1(4), I.2(2) becomes

$$M_i = \frac{1}{k_o^3 G^3} \left(\frac{w}{2\rho_o}\right)^{3/2} \cdot \frac{(k_o GR)^2}{2(I_1+I_2+I_3)}$$

$$= \left(\frac{w}{2\rho_o k_o^2 G^2}\right)^{3/2} \cdot \frac{(k_o GR)^2}{2(I_1+I_2+I_3)} \qquad \text{I.2(3)}$$

From equation 4.5(4)

$$\frac{I_1}{(k_o GR)^2} = \frac{1}{2G^2}\left(-\frac{G}{2} + \sqrt{\frac{G^2}{4} + GH}\right)\left(H + \frac{G}{2} - \sqrt{\frac{G^2}{2} + GH}\right)$$

$$= \frac{1}{2}\left(-\frac{1}{2} + \sqrt{\frac{1}{4} + \frac{H}{G}}\right)\left(\frac{H}{G} + \frac{1}{2} - \sqrt{\frac{1}{4} + \frac{H}{G}}\right)$$

$$= \frac{1}{2}\left(-\frac{1}{2} + \sqrt{\frac{1}{4} + \frac{H}{G}}\right)^3 \qquad \text{I.2(4)}$$

From equation 4.5(6)

$$\frac{I_2}{(k_o GR)^2} = \frac{\omega' R\theta_c}{3G^2}\left[\frac{G}{2\sqrt{\frac{G^2}{4} + GH}}\left(H + \frac{G}{2} - \sqrt{\frac{G^2}{4} + GH}\right)\right.$$

$$\left. + \left(-\frac{G}{2} + \sqrt{\frac{G^2}{4} + GH}\right)\left(1 - \frac{G}{2\sqrt{\frac{G^2}{4} + GH}}\right)\right] .$$

$$\frac{I_2}{(k_o GR)^2} = \frac{1}{3}\left[\frac{\omega' R\theta_c}{G}\right]\left[\frac{1}{2\sqrt{\frac{1}{4}+\frac{H}{G}}}\left(\frac{H}{G}+\frac{1}{2}-\sqrt{\frac{1}{4}+\frac{H}{G}}\right)\right.$$

$$\left.+\left(-\frac{1}{2}+\sqrt{\frac{1}{4}+\frac{H}{G}}\right)\left(1-\frac{1}{2\sqrt{\frac{1}{4}+\frac{H}{G}}}\right)\right] \qquad \text{I.2(5)}$$

Substituting from equation I.1(1), this becomes

$$\frac{I_2}{(k_o GR)^2} = \frac{1}{2}\left[\frac{\frac{w}{2\rho_o k_o^2 G^2} - \left(\frac{H}{G}+\frac{1}{2}-\sqrt{\frac{1}{4}+\frac{H}{G}}\right)}{1-\frac{1}{2\sqrt{\frac{1}{4}+\frac{H}{G}}}}\right]\left[\frac{1}{2\sqrt{\frac{1}{4}+\frac{H}{G}}}\left(\frac{H}{G}+\frac{1}{2}-\sqrt{\frac{1}{4}+\frac{H}{G}}\right)\right.$$

$$\left.+\left(-\frac{1}{2}+\sqrt{\frac{1}{4}+\frac{H}{G}}\right)\left(1-\frac{1}{2\sqrt{\frac{1}{4}+\frac{H}{G}}}\right)\right]$$

$$= \frac{1}{2}\left[\frac{w}{2\rho_o k_o^2 G^2} - \left(-\frac{1}{2}+\sqrt{\frac{1}{4}+\frac{H}{G}}\right)^2\right]\left[\frac{1}{2\sqrt{\frac{1}{4}+\frac{H}{G}}-1}\left(-\frac{1}{2}+\sqrt{\frac{1}{4}+\frac{H}{G}}\right)^2\right.$$

$$\left.+\left(-\frac{1}{2}+\sqrt{\frac{1}{4}+\frac{H}{G}}\right)\right]$$

$$= \frac{1}{2}\left[\frac{w}{2\rho_o k_o^2 G^2} - \left(-\frac{1}{2}+\sqrt{\frac{1}{4}+\frac{H}{G}}\right)^2\right]\left[\frac{\left(-\frac{1}{2}+\sqrt{\frac{1}{4}+\frac{H}{G}}\right)}{2}+\left(-\frac{1}{2}+\sqrt{\frac{1}{4}+\frac{H}{G}}\right)\right]$$

$$= \frac{3}{4}\left[\frac{w}{2\rho_o k_o^2 G^2} - \left(-\frac{1}{2}+\sqrt{\frac{1}{4}+\frac{H}{G}}\right)^2\right]\left[-\frac{1}{2}+\sqrt{\frac{1}{4}+\frac{H}{G}}\right]$$

I.2(6)

From equation 4.5(8)

$$\frac{I_3}{(k_o GR)^2} = \frac{1}{4}\left[\left(\frac{\omega' R\theta_c}{G}\right)^2\right]\left[\frac{G}{2\sqrt{\frac{G^2}{4}+GH}}\left(1 - \frac{G}{2\sqrt{\frac{G^2}{4}+GH}}\right)\right]$$

$$= \frac{1}{4}\left[\left(\frac{\omega' R\theta_c}{G}\right)^2\right]\left[\frac{1}{2\sqrt{\frac{1}{4}+H/G}}\left(1 - \frac{1}{2\sqrt{\frac{1}{4}+H/G}}\right)\right] \qquad \text{I.2(7)}$$

Substituting from equation I.1(1) this becomes

$$\frac{I_3}{(k_o GR)^2} = \frac{1}{4}\left\{\frac{3}{2}\left[\frac{\frac{w}{2\rho_o k_o^2 G^2} - \left(\frac{H}{G} + \frac{1}{2} - \sqrt{\frac{1}{4}+\frac{H}{G}}\right)}{1 - \frac{1}{2\sqrt{\frac{1}{4}+H/G}}}\right]\right\}^2$$

$$X\left[\frac{1}{2\sqrt{\frac{1}{4}+H/G}}\left(1 - \frac{1}{2\sqrt{\frac{1}{4}+H/G}}\right)\right]$$

$$= \frac{9}{16}\,\frac{\left[\frac{w}{2\rho_o k_o^2 G^2} - \left(-\frac{1}{2} + \sqrt{\frac{1}{4}+\frac{H}{G}}\right)^2\right]^2\left[\frac{1}{2\sqrt{\frac{1}{4}+H/G}}\right]}{\left(1 - \frac{1}{2\sqrt{\frac{1}{4}+H/G}}\right)}$$

$$= \frac{9}{16}\cdot\frac{\left[\frac{w}{2\rho_o k_o^2 G^2} - \left(-\frac{1}{2} + \sqrt{\frac{1}{4}+\frac{H}{G}}\right)^2\right]^2}{\left(2\sqrt{\frac{1}{4}+\frac{H}{G}} - 1\right)}$$

$$= \frac{9}{32}\cdot\frac{\left[\frac{w}{2\rho_o k_o^2 G^2} - \left(-\frac{1}{2} + \sqrt{\frac{1}{4}+\frac{H}{G}}\right)^2\right]^2}{\left(-\frac{1}{2} + \sqrt{\frac{1}{4}+\frac{H}{G}}\right)} \qquad \text{I.2(8)}$$

Adding together equations I.2(4), I.2(6), and I.2(8), we obtain

$$\frac{I_1+I_2+I_3}{(k_o GR)^2} = \frac{1}{2}\left(-\frac{1}{2}+\sqrt{\frac{1}{4}+\frac{H}{G}}\right)^3$$

$$+\frac{3}{4}\left[\frac{w}{2\rho_o k_o^2 G^2}-\left(-\frac{1}{2}+\sqrt{\frac{1}{4}+\frac{H}{G}}\right)^2\right]\left[-\frac{1}{2}+\sqrt{\frac{1}{4}+\frac{H}{G}}\right]$$

$$+\frac{9}{32}\left[\frac{w}{2\rho_o k_o^2 G^2}-\left(-\frac{1}{2}+\sqrt{\frac{1}{4}+\frac{H}{G}}\right)^2\right]^2\left[-\frac{1}{2}+\sqrt{\frac{1}{4}+\frac{H}{G}}\right]^{-1}$$

$$=\frac{1}{2}\left(-\frac{1}{2}+\sqrt{\frac{1}{4}+\frac{H}{G}}\right)\left\{\left(-\frac{1}{2}+\sqrt{\frac{1}{4}+\frac{H}{G}}\right)^2\right.$$

$$+\frac{3}{2}\left[\frac{w}{2\rho_o k_o^2 G^2}-\left(-\frac{1}{2}+\sqrt{\frac{1}{4}+\frac{H}{G}}\right)^2\right]$$

$$\left.+\frac{9}{16}\left[\frac{w}{2\rho_o k_o^2 G^2}-\left(-\frac{1}{2}+\sqrt{\frac{1}{4}+\frac{H}{G}}\right)^2\right]^2\left[-\frac{1}{2}+\sqrt{\frac{1}{4}+\frac{H}{G}}\right]^{-2}\right\}$$

$$=\frac{1}{2}\left(-\frac{1}{2}+\sqrt{\frac{1}{4}+\frac{H}{G}}\right)\left\{\left(-\frac{1}{2}+\sqrt{\frac{1}{4}+\frac{H}{G}}\right)+\frac{3}{4}\left[\frac{w}{2\rho_o k_o^2 G^2}-\left(-\frac{1}{2}+\sqrt{\frac{1}{4}+\frac{H}{G}}\right)^2\right]\left[-\frac{1}{2}+\sqrt{\frac{1}{4}+\frac{H}{G}}\right]^{-1}\right\}^2$$

$$=\frac{1}{2}\left(-\frac{1}{2}+\sqrt{\frac{1}{4}+\frac{H}{G}}\right)^{-1}\left\{\left(-\frac{1}{2}+\sqrt{\frac{1}{4}+\frac{H}{G}}\right)^2+\frac{3}{4}\left[\frac{w}{2\rho_o k_o^2 G^2}-\left(-\frac{1}{2}+\sqrt{\frac{1}{4}+\frac{H}{G}}\right)^2\right]\right\}^2$$

$$=\frac{1}{2}\left(-\frac{1}{2}\sqrt{\frac{1}{4}+\frac{H}{G}}\right)^{-1}\left[\frac{3}{4}\left(\frac{w}{2\rho_o k_o^2 G^2}\right)+\frac{1}{4}\left(-\frac{1}{2}+\sqrt{\frac{1}{4}+\frac{H}{G}}\right)^2\right]^2$$

$$=\frac{1}{32}\left(-\frac{1}{2}+\sqrt{\frac{1}{4}+\frac{H}{G}}\right)^{-1}\left[3\left(\frac{w}{2\rho_o k_o^2 G^2}\right)+\left(-\frac{1}{2}+\sqrt{\frac{1}{4}+\frac{H}{G}}\right)^2\right]^2$$

I.2(9)

Substituting this result into equation I.2(3) gives

$$M_i = \frac{16\left(\frac{w}{2\rho_o k_o^2 G^2}\right)^{3/2} \cdot \left(-\frac{1}{2} + \sqrt{\frac{1}{4} + \frac{H}{G}}\right)}{\left[3\left(\frac{w}{2\rho_o k_o^2 G^2}\right) + \left(-\frac{1}{2} + \sqrt{\frac{1}{4} + \frac{H}{G}}\right)^2\right]^2} \qquad \text{I.2(10)}$$

Substituting for H from equation 4.3(4) and neglecting v' gives

$$M_i = \frac{16\left(\frac{w}{2\rho_o k_o^2 G^2}\right)^{3/2} \cdot \left(-\frac{1}{2} + \sqrt{\frac{1}{4} + \frac{\omega' R \alpha_t'}{G} + \frac{V'}{G}}\right)}{\left[3\left(\frac{w}{2\rho_o k_o^2 G^2}\right) + \left(-\frac{1}{2} + \sqrt{\frac{1}{4} + \frac{\omega' R \alpha_t'}{G} + \frac{V'}{G}}\right)^2\right]^2} \qquad \text{I.2(11)}$$

Substituting for α_t' from equation 4.2(11) and collecting terms equation I.2(11) becomes

$$M_i = \frac{16\left(\frac{w}{2\rho_o k_o^2 G^2}\right)^{3/2} \cdot \left(-\frac{1}{2} + \sqrt{\frac{1}{4} k_o^2 s' \epsilon' \left(\frac{w}{2\rho_o k_o^2 G^2}\right) + \frac{V'}{G}}\right)}{\left[3\left(\frac{w}{2\rho_o k_o^2 G^2}\right) + \left(-\frac{1}{2} + \sqrt{\frac{1}{4} + k_o s' \epsilon' \left(\frac{w}{2\rho_o k_o^2 G^2}\right) + \frac{V'}{G}}\right)^2\right]^2}$$

which is equation 4.8(1).

Appendix II

Calculation of Parameters for an Example of a Tilt-Wing Convertiplane.

II.1.

For this example, values of the parameters assumed correspond approximately to values that might be typical of the military tactical transport now being developed by Hiller, Ryan, and Chance-Vought (Ref. 11), which was previously mentioned in paragraph 2.2(3). This aircraft is to be of tilt-wing design with four engines, so the following values of parameters have been assumed:

$w = 40$ lb/ft^2

$W = 7500$ lb/propeller-rotor

$V' = 250$ knots $= 423$ ft/sec.

$s' = 1.2$ (corresponds to 6000)

$\epsilon' = .125$ (corresponds to L/D = 8)

$a = 5.73$

$k_o = 1.0$

Since $w = \dfrac{W}{\pi R^2}$

$$R = \sqrt{\frac{W}{w\pi}} = \sqrt{\frac{7500}{40\pi}}$$

$$= 7.73 \text{ ft.}$$

From equation 6.2(1)

$$G = \frac{\frac{w}{2\rho_o k_o^2}\ (1 - k_o^2 s'\epsilon')}{V' - \sqrt{\frac{w}{2\rho_o k_o^2}}}$$

Using the assumed values listed above

$$\frac{w}{2\rho_o k_o^2} = \frac{40}{2X.002378} = 8400\ (\text{ft/sec})^2$$

$$\therefore \sqrt{\frac{w}{2\rho_o k_o^2}} = \sqrt{8400} = 92\ \text{ft/sec.}$$

$$s'\epsilon' = 1.2 \times .125 = .15$$

$$\therefore\ 1 - k_o^2 s'\epsilon' = 1 - .15 = .85$$

Substituting above we obtain

$$G = \frac{8400 \times .85}{423 - 92} = \frac{8400 \times .85}{331}$$

$$= 21.6\ \text{ft/sec.}$$

Since $G = \frac{1}{8}\, a\sigma\omega' R$

$$\frac{1}{8}\, a\sigma\omega' R = 21.6\ \text{ft/sec.}$$

Substituting for a, this reduces to

$$\sigma\omega'R = \frac{8 \times 21.6}{5.73}$$

$$= 30.1 \text{ ft/sec.} \qquad \text{II.1(1)}$$

With this criterion for relating σ and $\omega'R$, the induced figure of merit will be maintained at unity for the values of the parameters chosen.